J|A|C|S
ARTICLES
Published on Web 06/01/2002

Solution and Biologically Relevant Conformations of Enantiomeric 11-*cis*-Locked Cyclopropyl Retinals

Yukari Fujimoto, Nathan Fishkin, Gennaro Pescitelli, John Decatur, Nina Berova, and Koji Nakanishi*

Contribution from the Department of Chemistry, Columbia University, New York, New York 10027

Received January 16, 2002

Abstract: To gain information on the conformation of the 11-*cis*-retinylidene chromophore bound to bovine opsin, the enantiomeric pair (**2a** and **2b)** of 11-*cis*-locked bicyclo[5.1.0]octyl retinal (retCPr) **2** was prepared and its conformation was investigated by NMR, geometry optimization, and CD calculations. This compound is also of interest since it contains a unique moiety in which a chiral cyclopropyl group is flanked by triene and enal chromophores, and hence would clarify the little-known chiroptical contribution of a cyclopropyl ring linked to polyene systems. NMR revealed that the seven-membered ring of retCPr adopts a twist chair conformation. The NMR-derived structure constraints were then used for optimizing the geometry of **2** with molecular mechanics and ab initio methods. This revealed that enantiomer **2a** with a 11β,12β-cyclopropyl group exists as two populations of diastereomers depending on the twist around the 6-s bond; however, the sense of twist around the 12-s is positive in both rotamers. The theoretical Boltzmann-weighted CD obtained with the π-SCF-CI-DV MO method and experimental spectra were consistent, thus suggesting that the conjugative effect of the cyclopropyl moiety is minimal. It was found that only the β-cyclopropyl enantiomer **2a**, but not the α-enantiomer **2b**, binds to opsin. This observation, together with earlier retinal analogues incorporation results, led to the conclusion that the chromophore sinks into the N-terminal of the opsin receptor from the side of the 4-methylene and 15-aldehyde, and that the binding cleft accommodates 11-*cis*-retinal with a slightly positive twist around C12/C13. A reinterpretation of the previously published negative CD couplet of 11,12-dihydrorhodopsin also leads to a chromophoric C12/C13 twist conformation with the 13-Me in front as in **1b**. Such a conformation for the chromophore accounts for both the observed biostereoselectivity of retCPr **2a** and the observed negative couplet of 11,12-dihydro-Rh7.

Introduction

The bovine visual pigment rhodopsin (Rh), a prototypical G-protein coupled receptor (GPCR),[1−4] consists of opsin comprising 348 amino acids folded into seven transmembrane α-helices. The protein covalently binds the inverse agonist 11-*cis*-retinal (**la**, Figure 1) at the ϵ-amino group of Lys296 in helix G (Figure 2) through a protonated Schiff base (PSB) to form **1b**. Upon irradiation, dark state Rh undergoes 11-cis → trans photoisomerization to photo-Rh and batho-Rh, which is followed by thermal relaxation. Extensive low-temperature studies have identified the following intermediates: Rh (λ_{max} 500 nm) → photo-Rh (570 nm) → batho-Rh (543 nm) → lumi-Rh (497 nm) → meta-Rh I (meta-I, 480 nm) ↔ meta-Rh II (meta-II, 380 nm). The series of conformational changes[5] triggered by photoisomerization leads to meta-II, which activates the G protein (or transducin) giving rise to the enzymatic cascade responsible for rod vision.

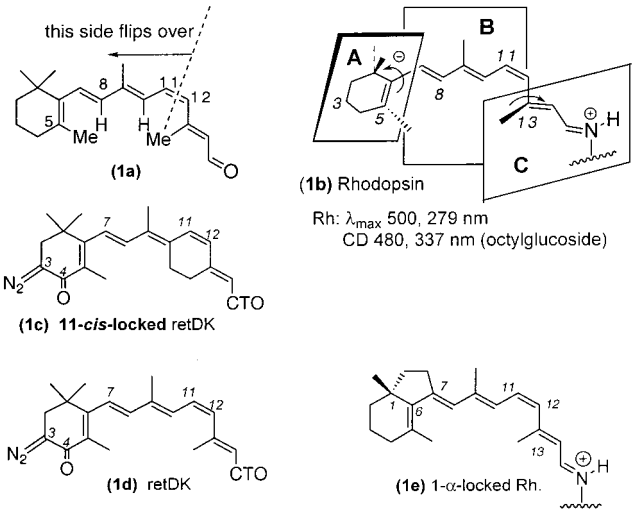

Figure 1. (**1a**) 11-*cis*-Retinal, (**1b**) rhodopsin, (**1c**) 11-*cis*-locked retDK, (**1d**) RetDK, and (**1e**) 1α-locked rhodopsin. In conversion of batho-Rh to lumi-Rh, the left side of chromophore **1a** flips over.

The recent 2.8 Å resolution X-ray crystal studies have elucidated the overall structural detail of rhodopsin (Figure 2), the first for any G protein coupled receptor (GPCR),[6,7] although further clarification of the chromophore conformation is still

* Corresponding author. E-mail: kn5@columbia.edu. Fax: (+1) 212-932-8273.

(1) Hargrave, P. A. *Invest. Ophthalmol. Visual Sci* **2001**, *42*, 3−9.
(2) Menon, S. T.; Han, M.; Sakmar, T. P. *Physiol. Rev.* **2001**, *81*, 1659−1688.
(3) Sakmar, T. P. *Prog. Nucleic Acid. Res. Mol. Biol.* **1998**, *59*, 1−34.
(4) Shichida, Y.; Imai, H. *Cell. Mol. Life. Sci.* **1998**, *54*, 1299−1315.
(5) Ishiguro, M. *J. Am. Chem. Soc.* **2000**, *122*, 444−45 1.

10.1021/ja020083e CCC: $22.00

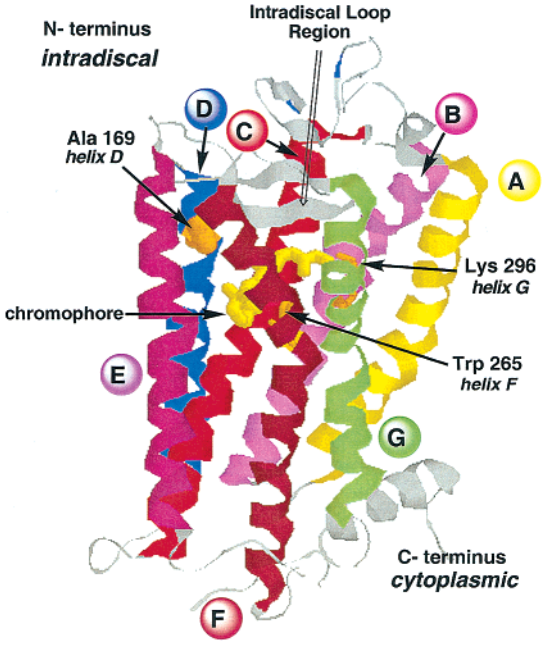

Figure 2. Rhodopsin crystal structure adopted from ref 2.

needed. Photoaffinity labeling studies performed on Rh with tritiated 11-*cis*-locked 3-diazo-4-ketoretinal **1c** showed that C3 of the chromophore solely cross-linked to helix F Trp265 close to the extracellular N-terminus (Figure 2).[8] Further affinity labeling studies performed with the respective transduction intermediates at low temperatures,[9,10] namely, at − 196 °C for batho, −80 °C for lumi, −40 °C for meta-I, and 0 °C for meta-II, using the unlocked retDK **1d** all yielded clear-cut results showing that in batho-Rh, C3 still cross-linked to Trp265 as with dark state Rh. However, the batho-Rh → lumi-Rh conversion results in a flip-over of the left side of the 11-*cis* molecule (see **1a**) so that C3 now becomes linked to Alal69 located on the outside rim of helix D (Figure 2); participation of a "Hula-Twist" might be conceivable for the isomerization.[11] This bridging to Ala169, which is the same in all subsequent intermediates, requires large helical movements and twists so that the cytoplasmic extramembrane loop conformation of meta-II activates the G protein.

The 11-*cis*-chromophore **1a** with the 6-*s*-*cis*[6,12,13] and 12-*s*-*trans* conformation[14,15] is twisted around the C6/C7 and C12/C13 bonds due to steric interactions between 5-Me/8-H and between 13-Me/10-H, respectively. The absolute sense of twists

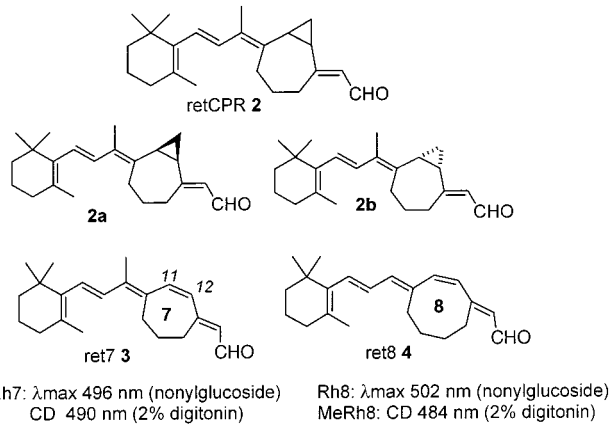

Figure 3. The structure of 11-*cis*-locked bicyclo[5.1.0]octyl retinal **2** and the seven- and eight-membered locked ret7 **3** and ret8 **4**.

around the 6-*s*-*cis* and 12-*s*-*trans* bonds have a direct bearing in regulating the movements of the chromophore after the initial 11-*cis* to *trans* photoisomerization has occurred. The 6-*s*-*cis* twist was recently established to be negative as depicted in **1b** (Figure 1) through binding studies of two enantiomeric 6-*s*-*cis*-locked retinoids. Only one of the enantiomers, namely, **1e**, bound to opsin to yield Rh**1e** with a CD similar to that of the native pigment. Moreover, the fact that Rh**1e** exhibited 80% of G protein binding activity suggests that the overall conformation around the 6-*s*-bond is retained during the transduction.[16]

On the other hand, the absolute sense of twist around the 12-*s*-bond has been less clear-cut. This has been investigated by analyzing the exciton-coupled CD of pigments incorporating 11,12-dihydroretinal and its 11-*cis*-locked analogue.[17] Studies have also been performed by NMR,[18,19] theoretical calculations,[20−23] and additional incorporation studies with 11-*cis*-locked retinoids,[24] but the results have been controversial.[25,26]

In the following we describe the solution conformation and spectral data of bicyclo[5.1.0]octyl retinals retCPr **2a** and **2b** with the 11-*cis* position locked into two enantiomeric forms due to the cyclopropyl group at C11 and C12 (Figure 3).[24,25] The UV/VIS and CD of the pigment incorporating ret7 **3** with the locked seven-membered ring (Figure 3, **3**) were similar to those of native Rh **1b** (Figure 1).[18] Hence retCPrs **2a** and **2b** were designed to further clarify the stereochemical requirements of the binding site, in particular the sense of twist around the 12/13 bond as the molecule enters the opsin binding site. In the reconstitution study of **2a** and **2b** with opsin, it was found that only the β-cyclopropyl analogue **2a**, but not its enantiomer

(6) Palczewski, K.; Kumasaka, T.; Hori, T.; Behnke, C. A.; Motoshima, H.; Fox, B. A.; Le Trong, I.; Teller, D. C.; Okada, T.; Stenkamp, R. E.; Yamamoto, M.; Miyano, M. *Science* **2000**, *289*, 739−745.
(7) Teller, D. C.; Okada, T.; Behnke, C. A.; Palczewski, K.; Stenkamp, R. E. *Biochemistry* **2001**, *40*, 7761−7772.
(8) Zhang, H.; Lerro, K. A.; Yamamoto, T.; Lien, T. H.; Sastry, L.; Gawinowicz, M. A.; Nakanishi, K. *J. Am. Chem. Soc.* **1994**, *116*, 10165−10173.
(9) Borhan, B.; Souto, M. L.; Imai, H.; Shichida, Y.; Nakanishi, K. *Science* **2000**, *288*, 2209−2212.
(10) Souto, M. L.; Borhan, B.; Nakanishi, K. *Methods Enzymol.* **2000**, *316*, 425−435.
(11) Liu, R. S. H.; Hammond, G. S. *Proc. Natl. Acad. Sci. U.S.A.* **2000**, *97*, 11153−11158.
(12) Mollevanger, L. C.; Kentgens, A. P.; Pardoen, J. A.; Courtin, J. M.; Veeman, W. S.; Lugtenburg, J.; de Grip, W. J. *Eur. J. Biochem.* **1987**, *163*, 9−14.
(13) Smith, S. O.; Palings, I.; Copie, V.; Raleigh, D. P.; Courtin, J.; Pardoen, J. A.; Lugtenburg, J.; Mathies, R. A.; Griffin, R. G. *Biochemistry* **1987**, *26*, 1606−1611.
(14) Chan, W. K.; Nakanishi, K.; Ebrey, T. G.; Honig, B. *J. Am. Chem. Soc.* **1974**, *96*, 3642−3644.
(15) Rando, R. *Chem. Biol.* **1996**, *3*, 255−262.
(16) Fujimoto, Y.; Ishihara, J.; Maki, S.; Fujioka, N.; Wang, T.; Furuta, T.; Fishkin, N.; Borhan, B.; Berova, N.; Nakanishi, K. *Chem. Eur. J.* **2001**, *7*, 4198−4204.
(17) Tan, Q.; Lou, J.; Borhan, B.; Karnaukhova, E.; Berova, N.; Nakanishi, K. *Angew. Chem., Int. Ed. Engl.* **1997**, *36*, 2089−2093..
(18) Han, M.; Smith, S. O. *Biochemistry* **1995**, *34*, 1425−1432.
(19) Verdegem, P. J.; Bovee-Geurts, P. H.; de Grip, W. J.; Lugtenburg, J.; de Groot, H. J. *Biochemistry* **1999**, *38*, 11316−11324.
(20) Buss, V.; Kolster, K.; Terstegen, F.; Vahrenhorst, R. *Angew. Chem., Int. Ed.* **1998**, *37*, 1893−1895.
(21) Buss, V.; Weingart, O.; Sugihara, M. *Angew. Chem., Int. Ed.* **2000**, *39*, 2784−2786.
(22) Buss, V. *Chirality* **2001**, *13*, 13−23.
(23) Kakitani, H.; Kakitani, T.; Yomosa, S. *J Phys. Soc. Jpn.* **1977**, *42*, 996−1004.
(24) Lou, J.; Hashimoto, M.; Berova, N.; Nakanishi, K. *Org. Lett.* **1999**, *1*, 51−54.
(25) Fujimoto, Y.; Xie, R.; Tully, S. T.; Berova, N.; Nakanishi, K. *Chirality* **2002**, *14*, 340−346.
(26) Kampermann, H.; Kolster, K.; Buss, V. *J. Mol. Model.* **2001**, *7*, 132−139.

2b, binds to give a pigment with a λ_{max} of 315 nm in contrast to 500 nm for the native rhodopsin pigment.[24,25] This observation together with the solution conformation of analogue **2a** leads to its biologically relevant conformation as it is incorporated into opsin (described below).

We first report the conformational analysis of bicyclo[5.1.0]-octyl ring moiety in retinoid **2**, particularly the seven-membered ring, by several NMR methods including measurements of nuclear Overhauser effect (NOE) and analysis of proton−proton vicinal spin-coupling constants ($^3J_{H,H}$).[27] The interpretation of NMR data is complicated by the fact that several conformations may exist in solution, each with a significant population. Since in the case of multiple conformers, NOE-derived distances can be weighted heavily toward shorter separations,[28,29] the NOE results needed to be corroborated by $^3J_{H,H}$ measurements. However, when protons are strongly coupled and show large second-order effects as is the case with the ^{1}H spectrum of retCPr **2**, $^3J_{H,H}$ are not easily extracted from E.COSY and related methods. We therefore resorted to coupled HSQC, which can eliminate these second-order effects under favorable conditions,[30] i.e., when the chemical shifts of carbons directly linked to strongly coupled protons are sufficiently different. We also report molecular modeling calculations of **2a** using the NMR-constrained ring system and then compare theoretical and experimental CD spectra to confirm the most probable conformation of the β-cyclopropyl enantiomer in solution.

Results and Discussion

Conformational Analysis by NMR. The 11-*cis*-locked bicyclo[5.1.0]octyl retinal **2** was synthesized and separated into enantiomers **2a** and **2b** by preparative chiral HPLC as described in a separate report.[25] ^{1}H NMR spectra of racemic **2** were measured at room temperature in benzene-d_6 and methanol-d_4 (Table 1); $CDCl_3$ was not used because of the instability of **2**, while the spectrum in acetonitrile-d_3 was difficult to interpret due to overlap of proton signals with residual solvent peaks. The chemical shifts of all protons summarized in Table 1 were assigned by DQF-COSY, NOESY, and HSQC. With respect to the methylene protons of the seven-membered ring, a deshielding effect was observed on the equatorial protons, H16a and H18a, in both solutions. The assignment of the H16a and H18a was also confirmed by NOESY data (Figure 4): there was an NOE between aldehyde proton H15 and H16a, but not H16b, and also an NOE between H8 and H18a, but not H18b.

NMR conformational analysis was focused on the bicyclo-[5.1.0]octyl ring system, especially the seven-membered ring because its conformation is crucial to determine the twist sense of the C12/13 bond in enantiomers **2a** and **2b**. NOESY spectra measured in benzene-d_6 and methanol-d_4 gave similar results (Figure 4). NOEs between methyl protons at C1 (H20 or H21) and both H7 and H8 indicated the nonplanarity around the C6/C7 bond. An NOE of medium intensity between H22 and H17a/H17b suggested a positive sense of twist around the C6/C7 bond; if the twist sense were negative, an NOE between H22 and H18 would be expected. The most noticeable NOE was that between

Table 1. ^{1}H Chemical Shifts of Analog **2** in Benzene-d_6 and Methanol-d_4

H atom position	δ (ppm)	
	benzene-d_6	methanol-d_4
2	1.51	1.49
3	1.60	1.64
4	1.97	2.02
7	6.29	6.15
8	6.52	6.40
11	1.59	2.23
12	1.30	2.02
14	6.08	6.10
15	9.90	9.90
16a	2.45	3.03
16b	1.24	1.83
17a	1.31	1.65
17b	1.21	1.57
18a	2.51	2.70
18b	1.80	2.06
19a	0.66	1.20
19b	0.79	1.47
20	1.12	1.02
21	1.13	1.01
22	1.79	1.69
23	1.87	2.01

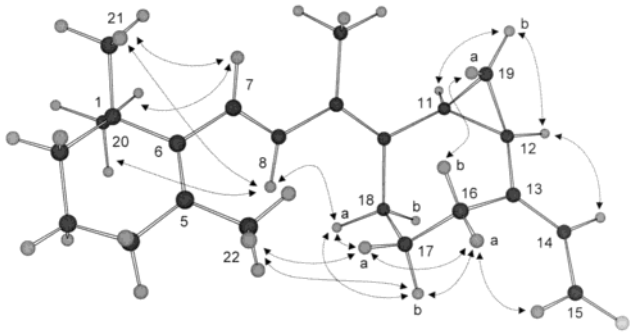

Figure 4. Through-space interactions in compound **2a** determined by NOESY of **2** in methanol-d_4 shown by dashed double-headed arrows.

H19a and H16b, which showed the seven-membered ring to adopt a twist chair conformation (Figure 4). However, it was necessary to consider the existence of multiple conformations for compound **2** because molecular mechanics calculations showed possible low-energy conformations in the boat form,[24] and not the twist chair. In cases when plural conformations exist, each with a significant population, an NOE cross-peak can have significant intensity even if it is due to a minor conformer. Therefore $^3J_{H,H}$ coupling constants of the seven-membered ring were also determined by means of coupled HSQC in benzene-d_6 solution (Figure 5) to confirm the NOE data. The coupled HSQC spectra facilitated the analysis of proton couplings by resolving cross-peaks arising from overlapping multiplets. Namely, clear-cut pure-phase spectra of each proton multiplet were obtained by extracting traces at the carbon frequency.

In benzene-d_6, protons 17a, 17b, and 16b had similar shifts (Table 1) and showed large second-order effects. Since H16b and H17b are attached to different carbons, coupled HSQC was able to simplify their analyses. The proton multiplets extracted from the cross-peak of C16, 17, and 18 are depicted in Figure 5. Although these multiplets are free from second-order effects, owing to the large number of proton−proton couplings (especially for H17a and H17b), the traces were still sufficiently complex that they needed to be simulated to determine the proton−proton couplings. The $^3J_{H,H}$ values are shown in Table

(27) Haasnoot, C. A. G.; De Leeuw, F. A. A. M.; De Leeuw, H. P. M.; Altona, C. *Org. Magn. Reson.* **1981**, *15*, 43−52.
(28) Neuhaus, D.; Williamson, M. P. *The Nuclear Overhauser Effect in Structural and Conformational Analysis*; John Wiley & Sons: New York, 2000.
(29) Post, C. B. *J Mol. Biol.* **1992**, *224*, 1087−1101.
(30) Simova, S. *Magn. Reson. Chem.* **1998**, *36*, 505−510.

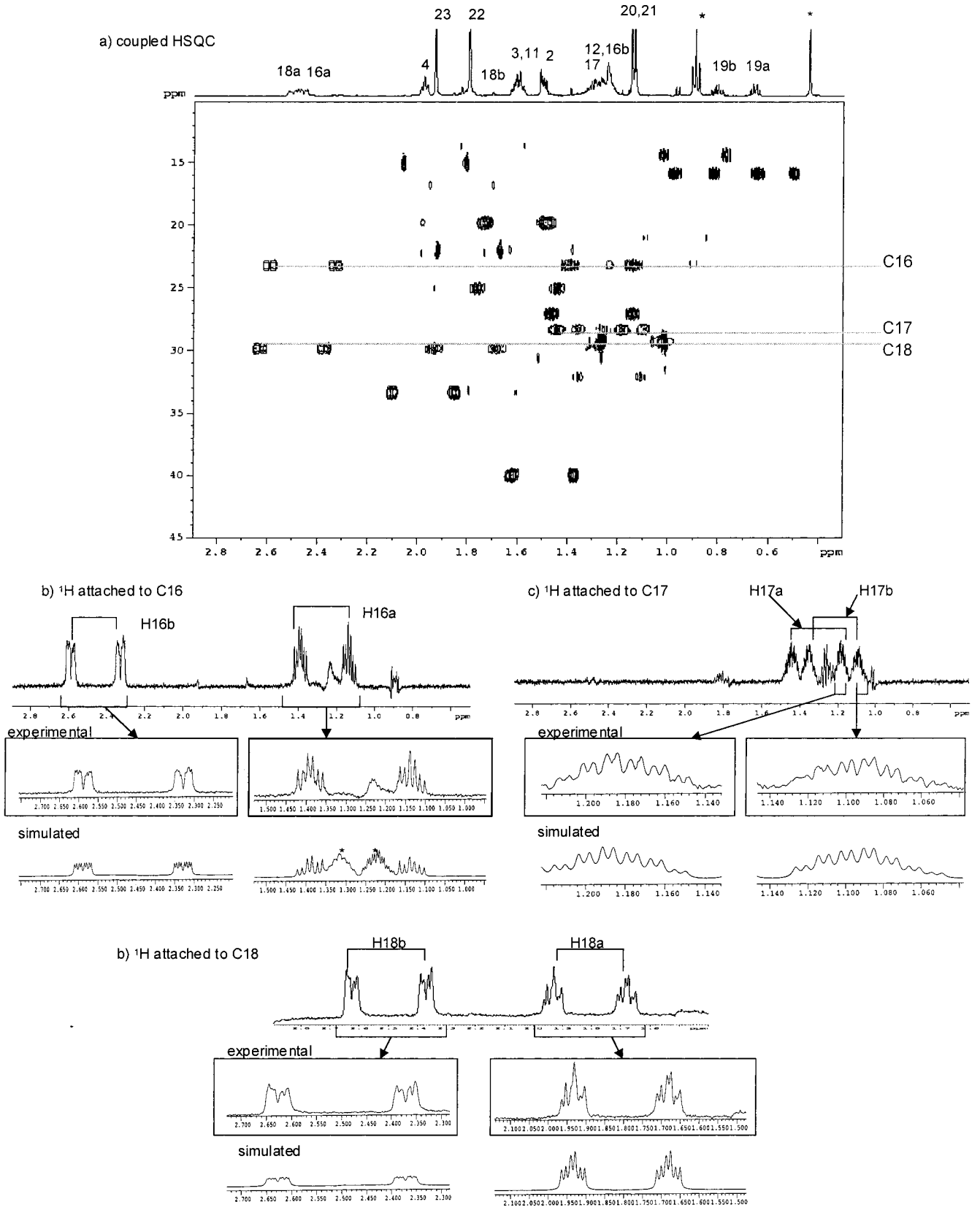

Figure 5. Coupled HSQC (a) and extracted proton spectra: (b) ^{1}H attached to C16, (c) ^{1}H attached to C17, and (d) ^{1}H attached to C18.

2 along with the estimated dihedral angles. Both NOEs and coupling constants suggested that the seven-membered ring of **2** adopts a twist chair conformation in which the sense of twist around the C12/C13 bond is positive in enantiomer **2a** (positive dihedral angle C11−C12−C13−C14 in Figure 4), and not negative as previously deduced.[24]

Molecular Modeling. The geometry of molecule **2** was calculated by constraining the conformation of the bicyclo[5.1.0]-

Table 2. The Coupling Constants of the Seven-Membered Ring Protons of Analog **2** in Benzene-d_6 and the Resulting Estimated Dihedral Angles for **2a**

coupled nuclei	coupling constants (Hz)	estimated dihedral angle (deg)
H18a/18b	13.21	110
H18a/17a	6.06	30
H18a/17b	2.69	50
H18b/17a	12.22	180
H18b/17b	6.03	50
H17a/17b	12.03	110
H17a/16a	2.61	50
H17a/16b	5.85	30
H17b/16a	5.97	30
H17b/16b	12.13	180
H16a/16b	13.25	110

octyl ring system as determined by NMR (Table 2). First we performed a Monte Carlo conformational search with MM3* force field incorporated into MacroModel 6.0, and chose the lowest energy structure with the seven-membered ring adopting the twist chair conformation, the most probable conformation derived by NMR. Geometry optimization of this conformer with B3LYP/6-31G in Jaguar 4.1 was then performed to obtain the local minimum. Starting from this optimized conformation, a fully relaxed scan of conformers rotated around the C6/C7 bond every 5°, using MM2* force field in Macromodel 6.0, showed the energy dependence on the C6/C7 torsion angle depicted in Figure 6a.

Geometry optimization with B3LYP/6-31G of the two minimum energy conformations resulted in two refined final conformations **2a(I)** and **2a(II)** depicted in Figure 6b with C6/C7 dihedral angles of +47.1° and −57.0°, respectively. The energies of conformers **2a(I)** and **2a(II)** were calculated at the B3LYP/6-31G** level to obtain more reliable conformational energies. It showed **2a(I)** had lower free energy by about 2.38 kJ/mol. In a previous paper, a possible lowest energy conformation **2a(III)** (Figure 6b) was suggested from a Monte Carlo conformational search with MM3*.[24] We also optimized conformation **2a(III)** with B3LYP/6-31G** (Figure 6b) and found it to be 4.5 kJ/mol higher in energy than conformer **2a(I)**. This result confirmed the twist-chair conformation of the seven-membered ring determined by NMR data and resulted in the two lowest energy conformations **2a(I)** and **2a(II)**.

Experimental and Theoretical CD of 2a. The absolute configuration of the pigment-forming β-cyclopropyl retinal analogue **2a** was established from the exciton coupled CD of the *p*-dimethylaminobenzoate of an intermediate allylic alcohol.[16] The λ_{max} of compound **2a** was 254 nm in MCH and 268 nm in methanol (Figure 6c). In MCH, a positive CD couplet 274 nm ($\Delta\epsilon$ +6.2)/241 nm ($\Delta\epsilon$ −10.4), A +16.6, arising from the interaction of $\pi-\pi^*$ transitions of the triene and enal chromophores, and a weak negative Cotton effect (CE) at 350 nm, attributed to the enal $n-\pi^*$, were observed. In methanol, a similar positive CD couplet at 281 nm ($\Delta\epsilon$ +8.5)/241 nm ($\Delta\epsilon$ −10.1), A +18.6, and a negative CE at 340 nm were observed, suggesting conformational similarities in the two solvents.

To reconcile the NMR determined conformation of the seven-membered ring with experimental CD data, the CD of retCPr **2a** was calculated with use of the lowest energy conformations **2a(I)** and **2a(II)**. The calculation was performed with the π-SCF-CI-DV MO method, taking into account the $\pi-\pi^*$ transitions of the two chromophores.[31] The results are shown in Figure 6d. It appears that a negative C5−C8 dihedral angle as in **2a(II)** gives rise to a negative bisignate CD, 275.4 nm ($\Delta\epsilon$ −18.6)/239.2 nm ($\Delta\epsilon$ +4.9), A −23.5. Yet, the lower energy conformation **2a(I)**, with a C5−C8 dihedral angle roughly equal in magnitude but opposite in sign to **2a(II)**, yields a comparatively strong positive bisignate feature 277.3 nm ($\Delta\epsilon$ +45.43)/238.2 nm ($\Delta\epsilon$ −20.9), A +66.33. *These results suggest that flexibility about the C6/C7 bond of CPRret7 in solution is a major factor controlling the observed CD.* In particular the C6/C7 torsion defines both the absolute sense of twist of the nonplanar C5−C10 triene moiety *and* the relative arrangement of the transition moments of the triene and the enal chromophores.

Not surprisingly, the CD calculated for the single conformations **2a(I)** and **2a(II)** cannot adequately describe the observed spectrum. Therefore, to take into account the conformational flexibility, the CD of each conformer within 3 kJ/mol of the local mimimum from each potential energy well (Figure 6a; 30 conformers total) were calculated and a weighted average of these spectra was obtained by applying a Boltzmann distribution. The resulting spectrum is depicted in Figure 6c, together with the experimental curves of **2a** in methylcyclohexane and methanol. The calculated spectrum shows a bisignate curve, 278 nm ($\Delta\epsilon$ +19.1)/241 nm ($\Delta\epsilon$ −10.4), A +29.5, which matches the experimental CD in sign, shape, and wavelength maxima, while it shows a larger amplitude for the long wavelength transition. The long wavelength $n-\pi^*$ transition of the aldehyde in the experimental curve at ca. 340 nm is not present in the calculated spectrum as only $\pi-\pi^*$ transitions are considered in these calculations. In addition, the theoretical spectrum resembles more closely the data in MCH than in the polar methanol solvent since the $\pi-\pi^*$ absorptions are red-shifted in methanol. It is worth noting that both molecular mechanics and the Boltzmann-weighted calculated CD suggest that a positive C6/C7 dihedral angle dominates in solution, a result that is experimentally corroborated by the medium-strength NOE between the C5 methyl group and the C17 protons on the seven-membered ring.

In addition to the energy considerations for conformation **2a(III)** (Figure 6b) described above, theoretical calculation of the corresponding CD spectrum, 284 nm ($\Delta\epsilon$ −21.9)/238 nm ($\Delta\epsilon$ +64.6), A −86.5, excludes this as the major conformer in solution. The crown conformation of **2a(III)** places the triene and enal chromophores relatively close to each other, which would explain the large amplitudes in the calculated CD. In sharp contrast to the −81° twist in **2a(III)**, the C11−C14 dihedral angle in **2a(I)** and **2a(II)** is +151.2°, which is consistent with the estimated acute angle of 44 ± 10° for retinal bound in opsin as determined by solid-state NMR distance measurements with ^{13}C-labeled retinoids.[19]

In principle, the CD of **2a** in the 200−320 nm region may result from the superimposition of several different origins of optical activity:[32] (a) exciton coupling between electric-dipole allowed $\pi-\pi^*$ transitions;[33] (b) inherent dissymmetry of the triene moiety, due to the C6−C7 twist;[34] (c) inherent dissym-

(31) Harada, N.; Nakanishi, K. *Circular Dichroic Spectroscopy Exciton Coupling in Organic Stereochemistry*; University Science Books: Mill Valley, CA, 1983.
(32) Mason, S. F. *Molecular Optical Activity and the Chiral Discrimination*; Cambridge University Press: Cambridge, UK, 1982.

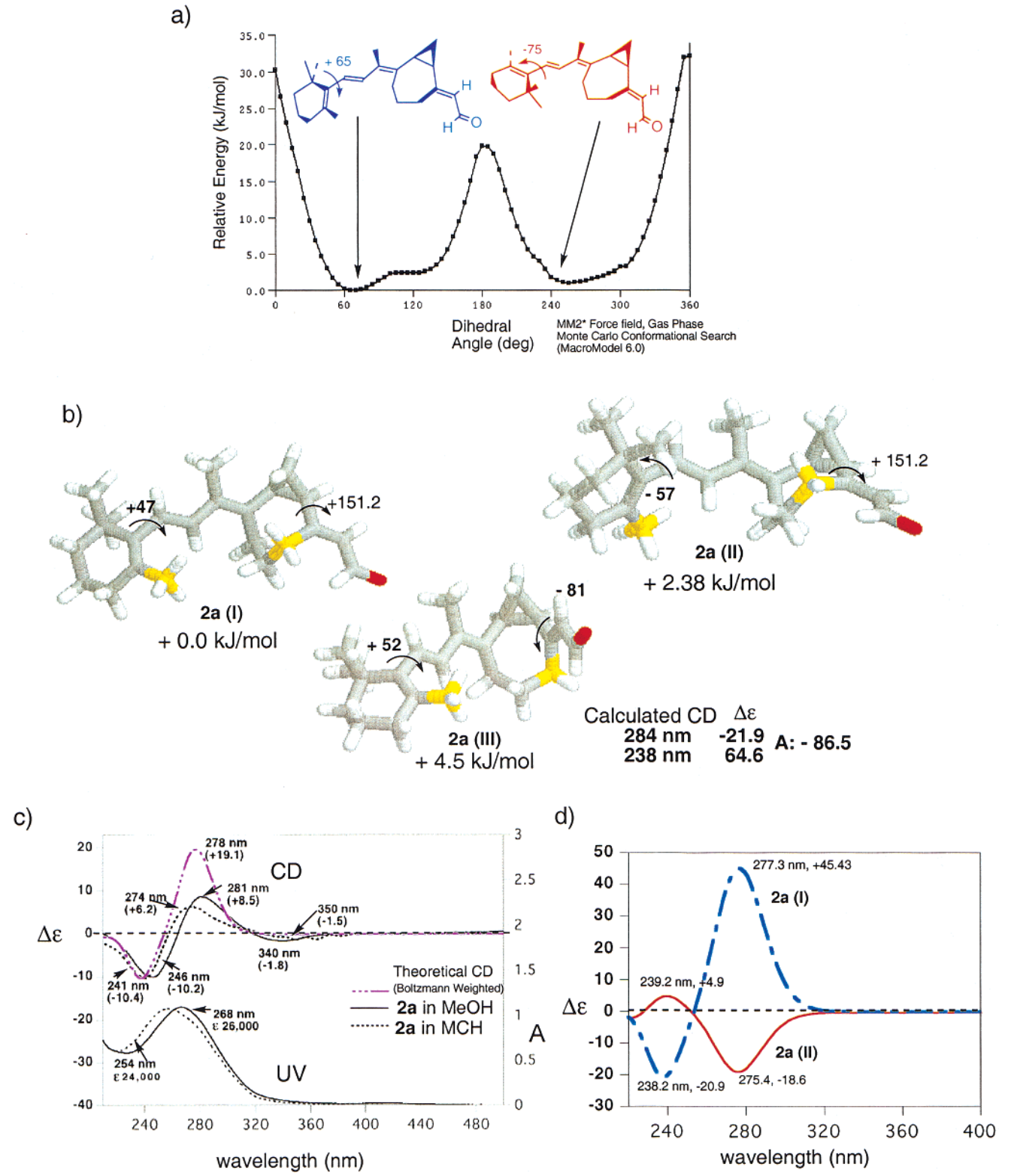

Figure 6. (a) MM2* torsional energy around the C6/7 dihedral angle in the twisted chair seven-membered ring conformation. (b) Calculated energies of **2a** with B3LYP/6-31G** (Jaguar 4.1). (c) Comparison of experimental (in methanol and methylcyclohexane, MCH) and Boltzmann-weighted calculated CD of **2a**. (d) Calculated CD spectra of conformations **2a(I)** and **2a(II)**.

metry of the triene−cyclopropane and the enal−cyclopropane conjugated systems;[35] (d) chirality of the entire chromophoric system whose conjugation is mediated by the cyclopropane ring; and (e) static and dynamic perturbation by substituents (primarily, the cyclopropane, the cycloheptane chain, and the C20−21 methyl groups) on the π chromophores.[32] Only the first two

(33) Berova, N.; Nakanishi, K. In *Circular Dichroism−Principles and Applications*; Berova, N., Nakanishi, K., Woody, R. W., Eds.; John Wiley & Sons: New York, 2000; pp 337−395.
(34) Salvadori, P.; Rosini, C.; Di Bari, L. *Conformation and chiroptical properties of dienes and polyenes*; Wiley: Chichester, UK, 1997; Vol. 1.
(35) Runge, W. *Chiroptical properties of cyclopropane derivatives*; Wiley: Chichester, UK, 1987; Vol. 1.

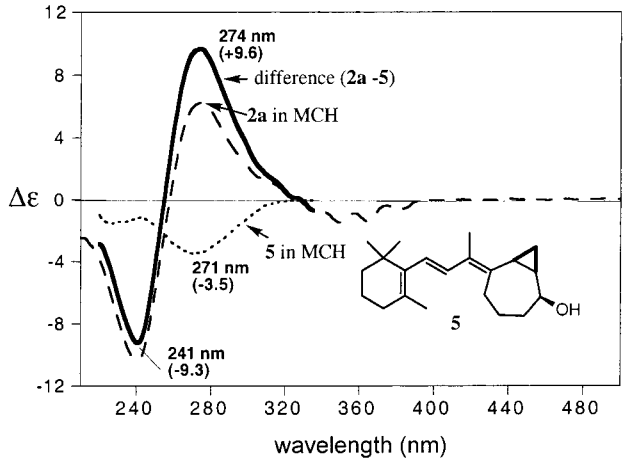

Figure 7. Subtraction of the CD spectrum of triene **5** from that of compound **2a**.

mechanisms can be directly taken into account by means of the π-SCF-CI-DV MO method. In particular, it needs additional adjustment to consider the well-known conjugative effects of the cyclopropane ring.[36] However, attempts to add homoconjugation properties to the C11 and C12 carbons of the cyclopropane ring by using a resonance integral ratio (β_{hc}/β (C═C)) between 1 and 30%[37] resulted in theoretical spectra with multiple and complex bands.

On the other hand, treatment of the cyclopropyl group as having no double bond character appeared to reproduce the experimentally observed bisignate curve. In both miminum energy conformations **2a(I)** and **2a(II)**, the C9−C10 double bond adopts a perpendicular orientation with respect to the plane bisecting the cyclopropane and passing through C11; in this situation, the triene−cyclopropane conjugation is negligible.[36] Among quantum mechanics semiempirical methods, INDO-based calculations have been applied to the study of cyclopropyl homoconjugation.[38] We performed ZINDO-S/CI calculations, using the lowest energy structure **2a(I)**, to estimate the extent of participation of cyclopropyl Walsh-type orbitals into the electronic transitions centered around 260 nm. An absorption band $\epsilon \approx 28\,000$ is calculated at 245 nm resulting from the superimposition of three transitions between 240 and 252 nm, which involve combinations of C5−C6 alkene, C7−C10 diene, and enal HOMO → LUMO. Although the enal MOs are mixed to some extent with cyclopropyl Walsh-type orbitals, the participation of the latter into the overall transition charge density is very modest (less than 1%).

The very good agreement between experimental and calculated CD spectra represents proof that the exciton coupling between triene and enal $\pi-\pi^*$ transitions and the inherent triene dissymmetry is dominant in defining the observed CD of **2a**. The relative contributions of these two mechanisms could be assessed by comparison with the CD of the monochromophoric alcohol **5**, which in MCH features a negative CE at 271 nm ($\Delta\epsilon$ −3.5), Figure 7; this value can be considered as an estimation of the CD due to the inherent chirality of the twisted triene. By subtracting the spectrum of **5** from that of **2a**, a clear

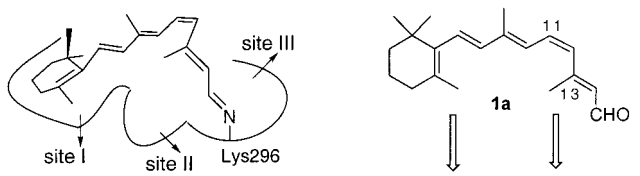

Figure 8. Mode of entry of chromophore into the binding site. Left: As the retinal ring moiety occupies the ionone binding site I and the aldehyde approaches Lys 296 at site III prior to PSB formation, the central polyene chain adjusts its conformation to fit into site II. Right: Arrows denote the direction of entry of 11-*cis*-retinal into the Rh binding site.

conservative exciton couplet is obtained at 274 nm ($\Delta\epsilon$ +9.6)/241 nm ($\Delta\epsilon$ −9.3), A +18.9, with extrapolated rotational strengths $R = +4.4$ and $-3.9\cdot10^{-39}$ cgs, respectively (Figure 7). Thus it can be concluded that the CD of **2a** is dominated by exciton coupling, as a parallel work inferred on a purely theoretical basis,[26] with only a minor contribution from the triene inherent chirality. A simple pictorial description of the observed exciton coupling, as well as coupled oscillators calculations, is hampered by the difficulty of depicting the triene $\pi-\pi^*$ transition in terms of a single electric dipole.

The CD (in MeOH) of **2a** butylamine Schiff base (λ_{max} 266 nm, ϵ 25 000) 279 nm ($\Delta\epsilon$ +8.7)/242 nm ($\Delta\epsilon$-14.6), A +23.3, and that of **2a** protonated butylamine Schiff base (λ_{max} 296 nm, ϵ 24,000) 304 nm ($\Delta\epsilon$ +16.3)/266 nm ($\Delta\epsilon$ −25.1), A +41.4, also exhibit exciton couplets.

On the Biologically Relevant Conformation of Retinal Analogues. On the basis of the solution conformation of analogue **2a** determined above, and taking into account previous incorporation data and the following reasonings, we consider that 11-*cis*-retinal and analogues enter the opsin extracellular N-terminus with a positive twist around the 12/13 bond (Figure 1, **1b**). (1) The opsin binding cavity incorporating the retinoids is divided into three binding domains, site I[39,40] for the cyclohexene ring, site II for the polyene chain, and site III for the PSB (Figure 8).[41] (2) Since ret7 **3** (Figure 3) yields pigment Rh7 almost as readily as native Rh from 11-*cis*-retinal **1a** and with similar UV/VIS maxima and CD to those of native Rh,[42] we assume that opsin has a potential cleft that readily incorporates these retinoids. (3) Incorporation studies with 11-*cis*-13-desmethylretinal (13dm), 11,12-dihydro-13dm, ret6, β-ionone, and other related compounds performed to elucidate the mechanism of *transient dark activity* of 13-desmethylretinal led to the conclusion that the chromophore enters the binding site by first occupying site I, followed by site III, and finally the central polyene site II (Figure 8).[41] (4) In contrast to ret7 **3**, ret8 **4** (Figure 3) with only one extra methylene group failed to bind smoothly to opsin, suggesting that the conformation of the ring portion of these analogues is a determinant for entering the binding cleft.[43] (5) The fact that only retCPr **2a**, not the enantiomeric **2b**, yielded a pigment shows that, as the retinoid enters the intradiscal N-terminal side of the receptor from the side indicated by arrows in Figure 8 (right structure), the conformation of the bottom side of the seven-membered ring

(36) Haumann, T.; Boese, R.; Kozhushkov, S. I.; Rauch, K.; De Meijere, A. *Liebigs Ann./Recl.* **1997**, 2047−2053.
(37) Harada, N.; Tamai, Y.; Takuma, Y.; Uda, H. *J. Am. Chem. Soc.* **1980**, *102*, *501*−*506*.
(38) Kispert, L. D.; Engelman, C.; Dyas, C.; Pittman, C. U., Jr. *J. Am. Chem. Soc.* **1971**, *93*, 6948−6953.
(39) Matsumoto, H.; Yoshizawa, T. *Nature* **1975**, *258*, *523*−*526*.
(40) Jager, S.; Palczewski, K.; Hofmann, K. P. *Biochemistry* **1996**, *35*, 2901−2908.
(41) Tan, Q.; Nakanishi, K.; Crouch, R. *J. Am. Chem. Soc.* **1998**, *120*, 12357−12358.
(42) Akita, H.; Tanis, S. P.; Adams, M.; Balogh-Nair, V.; Nakanishi, K. *J Am. Chem. Soc.* **1980**, *102*, 6370.
(43) Hu, S.; Franklin, P. J.; Wang, J.; Silva, B. E. R.; Derguini, F.; Nakanishi, K. *Biochemistry* **1994**, *33*, 408−416.

in **2a** can fit into the potential cleft in opsin, but this is not the case for the enantiomeric **2b**. Namely, we infer that the methylene portion of the seven-membered ring in **2a** is most likely predisposed with the proper conformation that can be accommodated by the receptor binding pocket. *This allows us to conclude that the retinoids enter the Rh binding site ftom the side of the 5-methyl and aldehyde groups* (see arrows in Figure 8, right structure).

Our current finding leading to a positive helicity (ca. 150°) of the chromophoric 12-*s* bond in the dark state receptor would appear to contradict an earlier conclusion in which 11,12-dihydro-ret7 gave a pigment with a negative exciton couplet, 297 nm (−6.5)/272 nm (+5.2), A −11.7.[17] At the time, this result was interpreted to mean that the 13-Me is in the rear of plane B (opposite twist sense to that depicted in Figure 1) since this conformation would qualitatively explain the observed negative CD exciton couplet. However, based on the exprimental observation that the C6/C7 twist is negative (determined with 6-*s*-*cis*-locked retinoids)[16] and that a negative C6/C7 twist and a positive C12/C13 twist as in **2a(II)** indeed yields a theoretical negative exciton couplet (Figure 6d), it now seems likely that 11,12-dihydro-ret7 initially enters opsin at site I with a negative C6/C7 twist and then enters site III with the *PSB in the rear of plane B, i.e., 13-Me in front. Such a conformation for the retinal chromophore would explain both the observed biostereoselectivity of retCPr* ***2a*** *and the observed negative couplet of 11,12-dihydro-Rh7*.[17]

The recent refinement of the rhodopsin X-ray data[7] reveals a C11−C12−C13−C14 dihedral angle of +151.6°, which is almost identical with that determined for **2a** in solution (Figure 6b). This observation further suggests that the retinal chromophore is transferred from the opsin binding cleft to the dark state retinylidene binding pocket with a retention of chirality around the 12-*s* bond. The chromophore in opsin seems to rest on the periphery of the N-terminal of the protein, embedded just below the intradiscal loop region, suggesting that 11-*cis* retinal does not have far to go to reach site III and form the PSB.

Conclusion

As mentioned above retCPr **2a** adopts a twist chair conformation of the seven-membered ring in solution. Dihedral angle drive about the C6/C7 bond and theoretical CD calculations show that **2a** exists as two diastereomeric populations centered around **2a(I)** and **2a(II)** (Figure 6a,b) with an approximately fixed orientation around C10−C13. In solution, native retinal shows no twist preference around the C6/C7 bond. However, with the pigment-forming 11β,12β-cyclopropyl enantiomer **2a**, there is a preference for a positive torsion around C6/C7 as in conformer **2a(I)**, presumably due to the steric interaction between the β-ionone *gem*-dimethyl group and C17 methylene of the seven-membered ring in conformer **2a(II)**. Thus, it appears that the experimental CD of **2a**, showing a positive CD couplet (Figure 6c), is due to the overriding positive couplet of conformer **2a(I)**. This unique model compound with a cyclopropyl group flanked by two chromophores exhibits a CD spectrum, the major component of which is consistent with an exciton coupling mechanism. Thus the contribution of the inherent triene chirality is small and that of cyclopropyl homoconjugation is seemingly negligible.

NMR and molecular modeling calculations show that the solution conformation of 11β,12β-11-*cis*-locked bicyclo[5.1.0]-octyl retinal **2a** has a positive helicity around the 12-*s* bond. The findings described above suggest that only retinoids capable of adopting a positive 12-*s* bond twist sink into the opsin extracelllular binding cleft, hence retinal **2a** can be incorporated but not retinal **2b**. The entering molecule first occupies site I (Figure 8), adopts a negative conformation around the 6-*s*-cis bond (Figure 1, **lb**),[16] then occupies site III, and this is followed by occupation of site II.[41]

Experimental Section

Materials and General Procedures. The 11-*cis*-locked bicyclo-[5.1.0]octyl retinal **2** was synthesized and separated into enantiomers **2a** and **2b** by enantioselective HPLC separation as described in a separate report.[25] The compounds were treated under dim light or sealed inside of amber glass. Benzene-d_6, methanol-d_4, and acetonitrile-d_3 (99.95 atom % Aldrich Chemical Co., Inc.) and benzene-d_6 (99.6 atom % D, Cambridge Isotope Laboratories, Inc.) were used as the solvents for NMR measurements. The solvents used for CD measurements were spectroscopic grade (Aldrich Chemical Co., Inc.).

NMR Measurements. All spectra were acquired on a Bruker DMX500 spectrometer equipped with a 5 mm triple resonance gradient probe. Chemical shifts are reported in parts per million (ppm) relative to TMS (δ), with coupling constants (J) in hertz (Hz).

NOESY spectra in methanol-d_4 were acquired in TPPI mode with the following parameters: spectral width 11 ppm, o1p 5.5 ppm, number of data points in F2 2K, and in F1 512 linear predicted to 1K and zero filled to 2K, 32 scans per increment, mixing time 0.5 s, relaxation delay 2 s, acquisition time 0.18 s, 90° pulse length, 8.1 μs processed with π/2 shifted sine-bell apodization.

NOESY spectra in benzene-d_6 were acquired with the same conditions, except for the number of data points in F2 8K and the acquisition time 0.747 s.

DQF-COSY were acquired in TPPI mode with the following parameters: spectral width 3 ppm, o1p 1.5 ppm, number of data points in F2 2K and in F1 512 zero-filled to 2K, 16 scans per increment, relaxation delay 2 s, acquisition time 0.68 s, 90° pulse length, 8.0 μs processed with π/2 shifted sine-bell apodization.

Refocused, gradient HSQC spectra were acquired by the sensitivity improved method,[44] using echo/antiecho selection for phase-sensitive detection. No decoupling was applied during acquisition for the coupled HSQC spectra. The following parameters were used: for the coupled HSQC spectral width 3 ppm (F2) and 40 ppm (F1), o1p 1.5 ppm (F2), o2p 30 ppm (F1), time domain points 4K (F2) and 64 (F1) zero-filled to 8K (F2) and 256 (F1), number of scans per increment 480, acquisition time 1.3 s, relaxation delay 0.3 s, 90° pulse length, 8.5 μs (^{1}H) 10 μs (^{13}C).

Gradient-selected E.COSY spectra were acquired by combining double (2QF), triple (3QF), and four quantum (4QF) COSY spectra.[45,46] The following parameters were used: spectral width 3 ppm, transmitter center 1.5 ppm, time domain points 4K (F2) and 512 (F1) zero filled to 8K and 1K, respectively, yielding a digital resolution of 0.18 and 1.46 Hz/pt, number of scans per increment 7, relaxation delay 1 s, 90° pulse length, 8.5 μs.

Proton spectra were simulated by using the gNMR program (Cherwell Scientific Ltd., now belonging to Adept Scientific). The procedure is as follows: initial guesses for chemical shifts and proton−proton couplings were used to generate a theoretical multiplet band shape. Transitions were assigned to observed peaks and then, using

(44) Kay, L. E.; Keifer, P.; Saarinen, T. *J. Am. Chem. Soc.* **1992**, *114*, 10663−10665.
(45) Willker, W.; Leibfritz, D.; Kerssebaum, R.; Lohman, J. *J Magn. Reson.* **1993**, *102*, 348.
(46) Griesinger, C.; Sorensen, O. W.; Ernst, R. R. *J Magn. Reson.* **1987**, *75*, 474−492.

least-squares methods, the theoretical band shape was fit to the experimental one. Then, transitions were reassigned and, if needed, the procedure was repeated until a best fit was obtained. Traces through carbons 16, 17, and 18 were extracted from the coupled HSQC and fit individually. Multiplets for protons 16a, 16b and 18a, 18b were simulated first. The resultant best-fit values were then used as a starting point for the simulation of protons 17a, 17b. As a final step, all proton multiplets were compared with theoretical spectra generated by the best-fit values.

Molecular Modeling and Computational Methods. Molecular mechanics calculations with MM2* and MM3* force fields and Monte Carlo conformational searches were executed with MacroModel 6.0 (Schrödinger, Inc., Portland, OR).

Nonempirical molecular modeling calculations were executed with Jaguar 4.1 (Schrödinger, Inc., Portland, OR) at the B3LYP level with 6-31G basis set including the geometry optimization, and then the energies of the obtained geometries were calculated at the B3LYP/6-31G* level.

UV/VIS, CD Measurements and Calculations. UV/VIS spectra were recorded on a Perkin-Elmer lambda 40 spectrophotometer, and reported as λ_{max} [nm] (ϵ_{max} [L mol^{-1} cm^{-1}]). The CD spectra were recorded on a JASCO-810 spectropolarimeter driven by a JASCO V500/FP-750 analysis program for Windows. The CD spectra were measured in millidegrees and normalized into $\Delta\epsilon_{max}$ [L mol^{-1} cm^{-1}] units.

SCF semiempirical ZINDO/S-CIS[47,48] calculations were executed with Hyperchem 6.1 (Hypercube, Inc.: Canada), using default parameters and convergence criteria. The highest 10 occupied and the lowest 10 virtual orbitals were included in the CI. UV/VIS curves were approximated by Gaussian distribution, with standard deviation of 2300 cm^{-1}.

The CD of each conformer was calculated according to the π-SCF-CI-DV MO method[31] in which only the $\pi-\pi^*$ transitions of the triene and enal chromophores were considered for the MO calculation (the CD computation program was provided by N. Harada, Sendai). The configuration interaction between 25 singly excited states of lower energy was included in the calculations. The atomic orbital parameters are as follows: for sp^2 carbons, Z(C) = 1.0, W(C) = −11.6 eV, (rr|rr)(C) = 11.13 eV, β(C−C, 1.34 Å) = −2.18 eV, $\langle\nabla\rangle$(C−C, 1.34 Å) = 4.701 × 10^7 cm^{-1}; carbonyl oxygens (sp^2), Z(O) = 2.0, W(O) = −17.28 eV, (rr|rr)(O) = 14.58 eV, β(C−O) = −2.54 eV, $\langle\nabla\rangle$(C−O) = 5.0 × 10^7 cm^{-1}. The electric repulsion integral (rr|ss) was estimated by the Nishimoto-Mataga equation.[49] The component CD curves were approximated by Gaussian distribution, and the standard deviation $\Delta\sigma$ values 2290 cm^{-1} were taken from the half value of the 1/e bandwidth of the observed UV spectrum of **2a** in MCH.

Acknowledgment. This research was supported by NIH grants GM 36564 and GM 34509. We gratefully acknowledge Professor Nobuyuki Harada, Tohoku University, for intensive discussions, Professor Jack Norton, Columbia University, for the use of gNMR, Drs. Jian-Guo Dong, Nasri Nesnas, Maria Wirstam (Professor Richard Friesner), and Jasna Klicic (Schrödinger, Inc.) for their suggestions and assistance for Jaguar calculations. We are also grateful for an NIH Vision training grant (EY 13933-01, to N.F.) and an Italian C.N.R. grant (203.03.26, to G.P.).

Supporting Information Available: ^{1}H NMR spectrum of **2** in benzene-d_6 and methanol-d_4 and NOESY spectrum of **2** in methanol-d_4 (PDF). This material is available free of charge via the Internet at http://pubs.acs.org.

JA020083E

(47) Ridley, J.; Zerner, M. *Theor. Chim. Acta* **1973**, *32*, 111−134.
(48) Ridley, J.; Zemer, M. C. *J. Mol. Spectrosc.* **1974**, *50*, 457−473.
(49) Nishimoto, K.; Mataga, N. Z. *Phys. Chem.* **1957**, *12*, 335.